

# UC Berkeley

## UC Berkeley Previously Published Works

### Title

Activity-Based Sensing with a Metal-Directed Acyl Imidazole Strategy Reveals Cell Type-Dependent Pools of Labile Brain Copper

### Permalink

<https://escholarship.org/uc/item/3640t4wp>

### Journal

Journal of the American Chemical Society, 142(35)

### ISSN

0002-7863

### Authors

Lee, Sumin  
Chung, Clive Yik-Sham  
Liu, Pei  
et al.

### Publication Date

2020-09-02

### DOI

10.1021/jacs.0c05727

Peer reviewed



# HHS Public Access

Author manuscript

*J Am Chem Soc.* Author manuscript; available in PMC 2021 May 02.

Published in final edited form as:

*J Am Chem Soc.* 2020 September 02; 142(35): 14993–15003. doi:10.1021/jacs.0c05727.

## Activity-Based Sensing with a Metal-Directed Acyl Imidazole Strategy Reveals Cell Type-Dependent Pools of Labile Brain Copper

**Sumin Lee**<sup>○</sup>,

Departments of Chemistry, University of California, Berkeley, California 94720, United States

**Clive Yik-Sham Chung**<sup>○</sup>,

Departments of Chemistry, University of California, Berkeley, California 94720, United States; School of Biomedical Sciences and Department of Pathology, The University of Hong Kong, Hong Kong, P.R. China

**Pei Liu,**

Departments of Chemistry, University of California, Berkeley, California 94720, United States

**Laura Craciun,**

Molecular and Cell Biology, University of California, Berkeley, California 94720, United States

**Yuki Nishikawa,**

Department of Synthetic Chemistry and Biological Chemistry, Graduate School of Engineering, Kyoto University, Kyoto 615-8510, Japan; ERATO Innovative Molecular Technology for Neuroscience Project, Japan Science and Technology Agency (JST), Kyoto 615-8530, Japan

**Kevin J. Bruemmer,**

Departments of Chemistry, University of California, Berkeley, California 94720, United States

**Itaru Hamachi,**

Department of Synthetic Chemistry and Biological Chemistry, Graduate School of Engineering, Kyoto University, Kyoto 615-8510, Japan; ERATO Innovative Molecular Technology for Neuroscience Project, Japan Science and Technology Agency (JST), Kyoto 615-8530, Japan

**Kaoru Saijo,**

Molecular and Cell Biology and Helen Wills Neuroscience Institute, University of California, Berkeley, California 94720, United States

**Evan W. Miller,**

---

**Corresponding Author: Christopher J. Chang** – [chrischang@berkeley.edu](mailto:chrischang@berkeley.edu).

<sup>○</sup>Author Contributions

These authors contributed equally to this work.

The authors declare no competing financial interest.

ASSOCIATED CONTENT

Supporting Information

The Supporting Information is available free of charge at <https://pubs.acs.org/doi/10.1021/jacs.0c05727>.

Experimental details including synthesis and characterization, metal reactivity and selectivity of CD probes, copper binding assay of CD433, and real-time imaging of cellular copper pools (PDF)

Complete contact information is available at: <https://pubs.acs.org/10.1021/jacs.0c05727>

Departments of Chemistry, Molecular and Cell Biology, and Helen Wills Neuroscience Institute, University of California, Berkeley, California 94720, United States

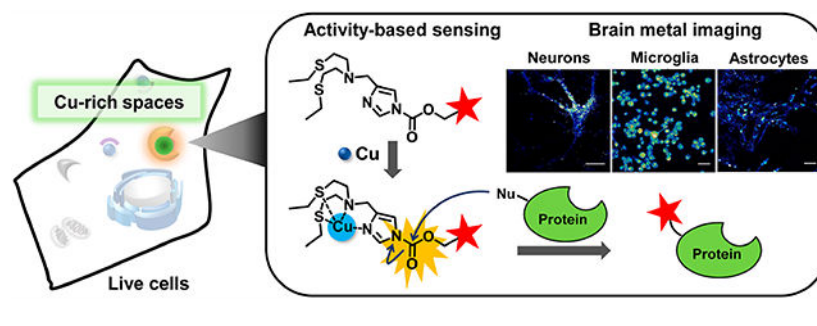
**Christopher J. Chang**

Departments of Chemistry, Molecular and Cell Biology, and Helen Wills Neuroscience Institute, University of California, Berkeley, California 94720, United States

**Abstract**

Copper is a required nutrient for life and particularly important to the brain and central nervous system. Indeed, copper redox activity is essential to maintaining normal physiological responses spanning neural signaling to metabolism, but at the same time copper misregulation is associated with inflammation and neurodegeneration. As such, chemical probes that can track dynamic changes in copper with spatial resolution, especially in loosely bound, labile forms, are valuable tools to identify and characterize its contributions to healthy and disease states. In this report, we present an activity-based sensing (ABS) strategy for copper detection in live cells that preserves spatial information by a copper-dependent bioconjugation reaction. Specifically, we designed copper-directed acyl imidazole dyes that operate through copper-mediated activation of acyl imidazole electrophiles for subsequent labeling of proximal proteins at sites of elevated labile copper to provide a permanent stain that resists washing and fixation. To showcase the utility of this new ABS platform, we sought to characterize labile copper pools in the three main cell types in the brain: neurons, astrocytes, and microglia. Exposure of each of these cell types to physiologically relevant stimuli shows distinct changes in labile copper pools. Neurons display translocation of labile copper from somatic cell bodies to peripheral processes upon activation, whereas astrocytes and microglia exhibit global decreases and increases in intracellular labile copper pools, respectively, after exposure to inflammatory stimuli. This work provides foundational information on cell type-dependent homeostasis of copper, an essential metal in the brain, as well as a starting point for the design of new activity-based probes for metals and other dynamic signaling and stress analytes in biology.

**Graphical Abstract**



**INTRODUCTION**

Copper is an essential element for human health.<sup>1</sup> Indeed, enzymes harness the potent redox activity of this metal nutrient to perform functions spanning energy generation, pigment synthesis, and epigenetic modifications.<sup>1-7</sup> Owing to the high metabolic and signaling needs of the brain, copper is found in particularly high concentrations in this organ,<sup>8-12</sup> where

work from our laboratory showed that activation of neurons causes a marked redistribution of cellular copper to affect the excitability of cultured neurons,<sup>13</sup> with subsequent studies identifying that these labile copper pools regulate spontaneous activity of circuits in retinal tissue<sup>12</sup> and sleep behavior in zebrafish models in vivo.<sup>14</sup> However, misregulation of copper homeostasis can lead to cellular malfunctions resulting from aberrant increases in reactive oxygen species (ROS) that can lead to oxidative damage to proteins, lipids, and DNA/RNA.<sup>15,16</sup> Such stress responses contribute to diseases including cancer,<sup>17–19</sup> neurodegenerative diseases such as Alzheimer's, Parkinson's, and Huntington's diseases,<sup>20–24</sup> and genetic disorders such as Menkes and Wilson's diseases.<sup>25–27</sup> These correlations are intriguing, but the underlying causal contributions of copper homeostasis to function and disease in the brain and central nervous system remain insufficiently understood. To this end, a number of chemical technologies have been developed to probe biological copper fluxes by molecular imaging, including fluorescent,<sup>11–14,18,28–47</sup> and magnetic resonance imaging (MRI),<sup>48–56</sup> and bioluminescent<sup>57</sup> copper indicators. These reporters can achieve high selectivity and signal-to-noise responses for copper ion imaging from cellular to tissue to whole animal settings. Application of these reagents, in conjunction with complementary biochemical, cellular, and animal studies, have given rise to the emerging concept of transition metal signaling, where such elements can reversibly modulate the activity of protein targets by fast and reversible binding beyond the active site.<sup>4,17,58,59</sup>

In this context, most fluorescent copper probes are designed to recognize labile copper ions based on thioether-rich receptors or tris[(2-pyridyl)methyl]amine (TPA) receptors.<sup>40</sup> These receptors have been exploited to trigger a fluorescent turn-on or ratiometric response by reversible coordination of copper ions or by activity-based sensing through irreversible uncaging of a fluorophore<sup>40,60–63,18</sup> or luciferin.<sup>57</sup> Despite advances in designing probes for studying copper biology, a gap in the field is to improve control over the localization of diffusible synthetic indicators to achieve higher spatial resolution for copper and related analytes of interest. To meet this need, we now present the design, synthesis, and biological applications of a new type of activity-based sensing (ABS) platform<sup>64,65</sup> for fluorescent copper detection using acyl imidazole bioconjugation chemistry. In ABS, the analyte is detected by an analyte-triggered reaction rather than a simple binding event, akin to activity-based protein profiling for reading out protein activity rather than protein abundance. We have prepared copper-directed acyl imidazole (CDAI or CD) fluorescent probes that feature a thioether NS2 receptor<sup>32,36,30,33</sup> bearing a fused acyl imidazole linked to coumarin (CD433) or Si-rhodamine (CD649) fluorophores, where copper binding increases the electrophilicity of the acyl imidazole unit for nucleophilic attack and covalent labeling of proximal proteins with the fluorescent dye. This approach is inspired by ligand-directed acyl imidazole (LDAI) reagents for proteomics and activity-based protein profiling (ABPP).<sup>66–72</sup> One of the advantages of utilizing this LDAI strategy for sensing and imaging purposes is to overcome a major challenge that small-molecule fluorescent probes can diffuse away from their target upon binding. CD probes address this problem by leveraging the direct coordination of Lewis acidic copper ions, resulting in covalent bond formation between fluorescent reporters and proximal proteins in the cell to preserve spatial information of localized copper hotspots by minimizing diffusion of the dye away from the site of the ABS reaction. A second advantage is, unlike existing activity-based sensing systems derived from

TPA that require both Cu(I) and O<sub>2</sub> to trigger a signal change, the CD probes can be activated directly by copper ions alone. The red-emissive CD probe CD649 was utilized to image increases and decreases in labile copper pools in live cells with exogenous copper supplementation or depletion, respectively, as well as monitor differences in labile copper status in genetic modified MEF cells with knockout of the ATP7A copper-exporter P-type ATPase compared to the wild-type congeners.

Moreover, to decipher fundamental copper biology in the central nervous system, CD649 was applied to characterize labile copper pools in the three major types of cells in the brain: neurons, astrocytes, and microglia. In primary cultured hippocampal neurons, CD649 revealed the translocation of labile copper from somatic cell bodies to the dendrites during neuronal depolarization. In parallel, CD649 identified global increases in labile copper in microglia and decreases in astrocytes during the inflammatory response. Taken together, this work provides a unique approach to direct activity-based sensing of copper that can retain spatial information with a modular design concept that applied to other biological analytes of interest. In addition, the foundational information on cell type-specific changes in labile copper offers a starting point for further investigations of copper biology in the brain and beyond to advance our understanding of transition metal signaling.

## RESULTS AND DISCUSSION

### Synthesis and Characterization of Copper-Directed Acyl Imidazole (CD) Probes for Activity-Based Sensing of Copper.

To develop a copper-responsive activity-based sensing probe that operates by proximal protein labeling, a thioether NS2 motif fused to imidazole was chosen as the copper recognition unit as inspired by previous copper-selective fluorescent<sup>4,11–13,28–32,41–43,58,73–77</sup> and MRI probes<sup>48,51–53</sup> as well as porous polymers for copper capture and detection.<sup>78</sup> The tripodal receptor **9** was synthesized in three steps. Dicarboxylic acid silicon-rhodamine **6** and its NHS ester **7** was prepared according to a reported procedure,<sup>79</sup> and NHS ester **7** was amide coupled to compound **10** to give copper-directed acyl imidazole 649 (CD649, Scheme 1). The coumarin derivative **11** was synthesized following published literature protocols<sup>66</sup> and conjugated to compound **9** to give CD433 (Scheme 1). The final CD probes were characterized by <sup>1</sup>H and <sup>13</sup>C{<sup>1</sup>H} NMR, LC-MS, and high-resolution MS.

For labeling proximal proteins in live cells in a copper-dependent manner, the CD probes should bind and react through accessible nucleophilic amino acids. To evaluate the reactivity and stability of the CD probes in vitro, the hydrolysis reaction of CD433 in the presence or absence of Cu(I) was monitored by liquid-chromatography in PBS buffer containing glutathione (2 mM). CD433 alone is stable in aqueous solutions as monitored for 4 h, but the introduction of copper promotes rapid reactivity at the carbamate unit of the acyl imidazole and hydrolysis with a 7.1-fold increase in product formation as found in LC chromatogram (Figure S1 of the Supporting Information, SI). Likewise, liquid chromatograms of the reaction between 5 μM CD649 and 2 equiv of Cu(I) in PBS in the presence of 5 molar equiv of L-serine methyl ester and 2 mM glutathione (GSH) showed complete conversion to the

copper-bound species and/or the copper-induced acyl transfer reaction product within 1 h (Figure 1a).

After 30 min, the intact CD649 probe disappeared to afford a product with a mass of 603  $m/z$  (Figure 1b), corresponding to the cleaved CD649 species with loss of the copper receptor and another product with a mass of 893  $m/z$  that corresponds to CD649 coupled to GSH, with a retention time at 7.4 min. (Figure 1c). Control experiments performed in the absence of amino acids revealed that CD649 does indeed fragment upon addition of copper ions; however, the resulting products were not detected at the retention time of 7.4 min, supporting the idea that nucleophilic amino acids are necessary to generate the copper-responsive reaction products (Figure S3). This activity-based sensing reaction is copper-selective, which is supported by liquid chromatography trace of CD probes incubated with other biologically relevant metal ions. Indeed, comparing the LC traces of CD649 with 10  $\mu\text{M}$   $\text{Na}^+$ ,  $\text{K}^+$ ,  $\text{Mg}^{2+}$ ,  $\text{Ca}^{2+}$ ,  $\text{Fe}^{3+}$ ,  $\text{Co}^{2+}$ ,  $\text{Ni}^{2+}$ ,  $\text{Cu}^+$ , or  $\text{Zn}^{2+}$  with L-serine methyl ester (25  $\mu\text{M}$ ) and 2 mM GSH in PBS, CD649 showed the conversion to 7.4 min retention time products only with copper addition (Figure 1d). After the metal selectivity was evaluated in aqueous conditions, we proceeded to test the copper-directed labeling strategy with lysozyme as a model protein owing to its commercial availability in large quantities (Figures 1e and S4). Lysozyme (1.55  $\mu\text{M}$ , 50  $\mu\text{L}$ ) was incubated with biologically relevant metal ions for 30 min at room temperature and then the premixed solutions were further incubated with 1  $\mu\text{M}$  of CD649 for 30 min. Fluorescent gel analysis showed that CD649 selectively labels the protein in case of Cu(I)/Cu(II) and the labeled band became significantly diminished upon addition of BCS (structure is shown at Figure 2b), supporting the notion that the nucleophilic amino acids on a protein surface were labeled with CD649 via acyl transfer reaction in the presence of copper ions (Figure 1e). We further checked the CD649 selectivity with HEK 293T lysates incubated with Cu(I) and Fe(II) prepared in the bioglove box, which exhibits the comparable labeling capability of CD649 toward Cu(I)/Cu(II) labeled protein (Figure S5). To investigate any oxidation state specificity of CD probes toward copper, lysozyme in PBS was premixed with Cu(I)/Cu(II) for 5 min, followed by incubation with CD649 for 2 h under a  $\text{N}_2$  atm so that no oxidation of Cu(I) would occur. Similar fluorescence intensities of labeled lysozyme were found in the presence of Cu(I) and Cu(II) ions, respectively (Figure S10), indicating that the CD probes are responsive toward both Cu(I) and Cu(II) ions.

In addition, we found a linear increase in fluorescence intensity of HEK 293T cell lysates labeled by CD649 with increasing copper ion concentration, and a limit of detection is found to be 0.864 nM (Figure S8). These data suggest that protein labeling by the CD probes is highly sensitive and dose-dependent toward copper. A dose-dependent increase in fluorescence intensity of lysozyme labeled by CD649 was also found with increasing copper, whereas changes in fluorescence intensities with fixed copper ion concentrations and varying lysozyme concentrations were much smaller and plateaued at high lysozyme concentrations (Figure S9). In view of the much higher concentrations of protein compared to CD probe in biological environments, the effect of changes in protein concentration on observed fluorescence should be minimal. Finally, to evaluate the relative copper affinity of the CD probes, CD433 was employed in a competitive copper binding assay with the reported copper fluorescent probe, CSR1, whose emission profile does not overlap with that

of CD433.<sup>80,81</sup> In these experiments, CD433 (0–5 equiv) was continuously added to a pH 7.0 buffer solution (25 mM HEPES) containing the copper-complexed form of CSR1, which is reported to have a dissociation constant ( $K_d$ ) with Cu(I) of  $2 \times 10^{-13}$  M.<sup>59</sup> The solution containing the probes was excited at 608 nm, where CD433 does not absorb, and as the concentration of CD433 was increased, the observed fluorescence intensity derived from CSR1 significantly decreased, suggesting that CD433 can compete with CSR1 for copper binding and is capable of displacing the copper ion from this Si-rhodol sensor (Figure S6). As CSR1 is capable of monitoring dynamic changes in labile copper pools in live cells as shown by identification of copper fluxes induced by lipolysis,<sup>59</sup> this set of experiments presages that the CD platform should have sufficient affinity for copper in related cellular assays.

### Live-Cell Imaging of Labile Copper Pools with CD649 Under Situations of Copper Elevation or Depletion.

After establishing that CD probes are sensitive to copper with high metal selectivity and can label a model protein by SDS-PAGE analysis with a fluorogenic readout, we next tested the ability of this ABS platform to respond to changes in labile copper levels in living cells. Specifically, we applied CD649 to live HEK 293T cells and cellular copper levels were perturbed by preincubating with Cu(gtsm) to increase intracellular copper levels and BCS to decrease intracellular copper levels. As anticipated, we observed a robust 2-fold increase in fluorescence intensity following treatment with  $2 \mu\text{M}$  Cu(gtsm), with the labeling being distributed evenly across the cytosol as compared to the punctate staining pattern observed under basal conditions. In contrast, HEK 293T cells pretreated with  $200 \mu\text{M}$  BCS for 10 h to induce copper depletion displayed a significant decrease in fluorescence intensity as compared to control cells as shown with CD649 imaging (Figure 2a), establishing that this ABS probe can monitor changes in labile copper levels in live cells, with fairly low cell toxicity as indicated by PrestoBlue assay (Figure S11). Likewise, CD433 was incubated with HEK 293T cell lysates in the presence of 1 equiv of Cu(I), and fluorescent intensity was measured at different incubation times up to 120 min. Those experiments show that the integrated fluorescence linearly increased and the fluorescence was quenched by preincubation with BCS (Figure S7), which confirms the copper-responsiveness of this probe. Next, we sought to evaluate the ability of CD649 to assay labile copper pools in genetic models of copper misregulation. In particular, we focused on matched cell lines with different levels of ATP7A, a copper-translocating P-type ATPase that regulates cellular copper pools by mediating cellular copper egress and secretory function. Indeed, mutations in the copper transporters ATP7A and ATP7B are at the heart of genetic disorders of copper homeostasis.<sup>26,82–84</sup> In particular, Menkes disease is derived from a loss of ATP7A function with systemic copper misregulation leads to hyperaccumulation of liver copper.<sup>85</sup> As anticipated, CD649-stained ATP7A knockout (KO) cells showed significantly higher levels of fluorescence compared to control ATP7A wild-type (WT) cells, revealing that CD649 can indeed detect elevated levels of labile copper in ATP7A KO cells, presumably due to the deficiency in cellular copper export (Figure 2d,e). Furthermore, both WT and KO cells showed an increase in fluorescence signal following incubation with Cu(gtsm) in a time- and dose-dependent manner, which can be attenuated by the addition of the copper chelator BCS

(Figure 2b). These data validate that CD649 can detect changes in labile copper levels with pharmacological and/or genetic manipulation.

### CD649 Enables Activity-Based Sensing of Copper in Major Brain Cell Types.

After confirming that CD649 can monitor changes in labile copper pools in mammalian cell line models, we then moved on to apply this new chemical tool to probe labile copper pools relevant to the brain and central nervous system. Indeed, copper homeostasis has profound effects in the brain as a neuromodulator in healthy states<sup>12,14,86–89</sup> and as a mediator of neuroinflammation and neurotoxicity in aging and disease states.<sup>6,14,90–93</sup> In this context, previous work from our laboratory using a combination of X-ray fluorescence microscopy (XRFM) and a reversible binding-based BODIPY fluorescent probe for copper (CS3) identified that neuronal activity triggers significant movements of labile copper pools from the soma to peripheral neuronal processes.<sup>13</sup> Here, we sought to expand on this observation by providing foundational information on labile copper pools in three main types of cells in the brain for comparison: neurons, astrocytes, and microglia. Starting with neurons, CD649 revealed punctate staining localized primarily to the soma of cultured primary hippocampal neurons in their resting state (Figure 3b). Activation and depolarization of these cultures by 50 mM KCl for 2 min,<sup>13</sup> or glutamate/glycine (50  $\mu$ M/5  $\mu$ M),<sup>8</sup> or electrostimulated (3000 evoked action potentials at a frequency of 20 Hz),<sup>94,95</sup> followed by staining with 1  $\mu$ M CD649, showed a significant redistribution of labile copper pools from somatic cell bodies to peripheral locations, in agreement with previous XRFM/CS3 data.<sup>13</sup> The percentage of CD649-stained neurons showing redistributed copper ions at least one cell body away from the center of the neuron was calculated, revealing that depolarized neurons have a 2-fold increase relative to resting neurons (Figure 3c), consistent with soma to dendrite copper pool redistribution. We also applied CD649 to real-time monitoring of labile copper pools in hippocampal neurons, showing punctate localization of labile copper in somatic cell bodies in neurons in their resting state with loss of these puncta upon application of a depolarization stimulus (Figure S12).

Next, we sought to characterize labile copper pools in astrocyte and microglia, as these cell types in the brain influence neurogenesis, angiogenesis, immune response, and synaptogenesis.<sup>96</sup> In particular, astrocytes have been reported as key regulators of brain copper homeostasis as they can efficiently acquire, store, and export copper owing to their high resistance to copper toxicity.<sup>96,97</sup> However, microglia are the major resident immune cells in the brain, producing factors that influence surrounding astrocytes and neurons and promoting neuron survival as well as synaptic pruning,<sup>97–99,96</sup> with less known about their copper biology. As both of these cell types are involved in inflammation, we utilized CD649 to probe changes in labile copper pools in human astrocyte (HA) and microglia SIMA9 cell lines in response to inflammatory stimuli. Cells were pretreated with inflammatory activators such as tumor necrosis factor alpha (TNF- $\alpha$ ), interleukin-1 alpha (IL-1 $\alpha$ ), lipopolysaccharide (LPS), or CpG oligodeoxynucleotides (ODN), washed and then stained with 5  $\mu$ M CD649. CD649 revealed labile copper pools localized in a punctate pattern within human astrocytes in their resting state. Stimulation with TNF- $\alpha$  and IL-1 $\alpha$  triggers a loss of punctate staining over increased inflammatory response (Figure 4a and b). The decrease in fluorescence signals measured by CD649 was supported by complementary



ICP-MS measurements of total cellular copper to phosphorus ratios showing expected decreases in the response to TNF- $\alpha$  and IL-1 $\alpha$  inflammatory stimuli (Figure 4c), suggesting a reduction and/or relocalization of labile copper pools. In contrast, microglia SIMA9 cells showed an increase in their labile copper pools in the response to inflammatory stimuli such as LPS and ODN compared to their basal state as monitored by CD649 imaging (Figure 4d and e). The increases in labile copper-dependent fluorescence signals were also supported by complementary ICP-MS measurements of total cellular copper (Figure 4f). The observed increase in the microglial labile copper pool under inflammatory stimuli is in line with a previous study reporting increased expression of ATP7A of the microglia cells in the response to the pro-inflammatory response.<sup>100-102</sup> The rise in ATP7A leads to increased copper uptake and elevated expression of the CTR1 copper importer to expand the overall labile copper pool.<sup>101</sup> Taken together, these data showcase the utility of CD649 for activity-based sensing of copper applied to reveal basic information on labile copper pools and their distinct dynamics in various brain cell types.

## CONCLUSIONS

To close, we have described the design, synthesis, and characterization of a unique platform for activity-based sensing (ABS) of copper by exploiting copper-dependent bioconjugation chemistry of acyl imidazole electrophiles. CD probes respond in a copper-dependent manner by increased covalent labeling of the dye with proximal proteins in cells at sites with elevated labile copper pools, which minimizes dye diffusion away from copper hotspots and preserves spatial information. This ABS strategy utilizes direct copper binding to trigger a fluorogenic response and does not require a metal- and oxygen-dependent reaction, offering an advantage over previous TPA-derived ABS probes. CD649 is capable of imaging changes in labile copper pools in HEK 293T and MEF cells with pharmacological copper supplementation and depletion, as well as detect elevations in endogenous levels of labile copper accumulation caused by knockout of the ATP7A copper exporter in MEF cell models. Moreover, we applied CD649 to characterize labile copper pools in the three main cell types in the brain: neurons, astrocytes, and microglia. In cultured primary hippocampal neurons, CD649 can track redistributions of labile copper pools from somatic cell bodies to peripheral processes upon depolarization. This probe also reveals distinct cell-specific responses in labile copper dynamics with inflammatory stimuli, where inflammation triggers relocation of labile copper in astrocytes and a labile copper increase in microglia. We speculate that the opposing dynamics of labile copper in these two cell types may contribute to neuroinflammatory reactions, where labile copper contraction in astrocytes is compensated by labile copper expansion in microglia as signal to communicate between cell types. Such crosstalk could serve as a neuroprotective mechanism in neurodegenerative disease. Current efforts are geared toward expanding the palette of ABS probes that operate by dual sensing/bioconjugation mechanisms for dual imaging/proteomics purposes, as well as applying CD649 and related chemical tools to decipher the biology of metals in the brain and beyond. We anticipate that such activity-based reagents will be of value in providing foundational information on the continuum between metal signaling and metal metabolism.

## Supplementary Material

Refer to Web version on PubMed Central for supplementary material.

## ACKNOWLEDGMENTS

We thank the NIH (GM 79465 to C.J.C. and R35 GM119855 to E.W.M.) for support of this work. C.Y.-S.C thanks the Croucher Foundation for a postdoctoral fellowship. P.L. was supported by a graduate fellowship from A\*STAR, Singapore. K.S. thanks the NIH (1R01HD09203) and Pew Scholarship. We thank Alison Killilea, Carissa Tasto, and Molly Fischer of the UC Berkeley Cell Culture Facility for cell culture support and thank Stefan Schmollinger at Sabeeha Merchant lab at UC Berkeley for ICP-MS measurement.

## REFERENCES

- (1). Lippard SJ; Berg JM Principles of Bioinorganic Chemistry; University Science Books: Mill Valley, CA, 1994.
- (2). Davis AV; O'Halloran TV A Place for Thioether Chemistry in Cellular Copper Ion Recognition and Trafficking. *Nat. Chem. Biol* 2008, 4 (3), 148–151. [PubMed: 18277969]
- (3). Boal AK; Rosenzweig AC Structural Biology of Copper Trafficking. *Chem. Rev* 2009, 109 (10), 4760–4779. [PubMed: 19824702]
- (4). Chang CJ Searching for Harmony in Transition-Metal Signaling. *Nat. Chem. Biol* 2015, 11 (10), 744–747. [PubMed: 26379012]
- (5). Guengerich FP Introduction to Metals in Biology 2018: Copper Homeostasis and Utilization in Redox Enzymes. *J. Biol. Chem* 2018, 293 (13), 4603–4605. [PubMed: 29425098]
- (6). Ackerman CM; Chang CJ Copper Signaling in the Brain and Beyond. *J. Biol. Chem* 2018, 293 (13), 4628–4635. [PubMed: 29084848]
- (7). Hunsaker EW; Franz KJ Emerging Opportunities To Manipulate Metal Trafficking for Therapeutic Benefit. *Inorg. Chem* 2019, 58 (20), 13528–13545. [PubMed: 31247859]
- (8). Schlieff ML NMDA Receptor Activation Mediates Copper Homeostasis in Hippocampal Neurons. *J. Neurosci* 2005, 25 (1), 239–246. [PubMed: 15634787]
- (9). Gaggelli E; Kozlowski H; Valensin D; Valensin G Copper Homeostasis and Neurodegenerative Disorders (Alzheimer's, Prion, and Parkinson's Diseases and Amyotrophic Lateral Sclerosis). *Chem. Rev* 2006, 106 (6), 1995–2044. [PubMed: 16771441]
- (10). Barnham KJ; Bush AI Biological Metals and Metal-Targeting Compounds in Major Neurodegenerative Diseases. *Chem. Soc. Rev* 2014, 43 (19), 6727–6749. [PubMed: 25099276]
- (11). Que EL; Domaille DW; Chang CJ Metals in Neurobiology: Probing Their Chemistry and Biology with Molecular Imaging. *Chem. Rev* 2008, 108 (5), 1517–1549. [PubMed: 18426241]
- (12). Dodani SC; Firl A; Chan J; Nam CI; Aron AT; Onak CS; Ramos-Torres KM; Paek J; Webster CM; Feller MB; Chang CJ Copper Is an Endogenous Modulator of Neural Circuit Spontaneous Activity. *Proc. Natl. Acad. Sci. U. S. A* 2014, 111 (46), 16280–16285. [PubMed: 25378701]
- (13). Dodani SC; Domaille DW; Nam CI; Miller EW; Finney LA; Vogt S; Chang CJ Calcium-Dependent Copper Redistributions in Neuronal Cells Revealed by a Fluorescent Copper Sensor and X-Ray Fluorescence Microscopy. *Proc. Natl. Acad. Sci. U. S. A* 2011, 108 (15), 5980–5985. [PubMed: 21444780]
- (14). Xiao T; Ackerman CM; Carroll EC; Jia S; Hoagland A; Chan J; Thai B; Liu CS; Isacoff EY; Chang CJ Copper Regulates Rest-Activity Cycles through the Locus Coeruleus-Norepinephrine System. *Nat. Chem. Biol* 2018, 14 (7), 655–663. [PubMed: 29867144]
- (15). Halliwell B; Gutteridge JMC [1] Role of Free Radicals and Catalytic Metal Ions in Human Disease: An Overview In *Methods in Enzymology; Oxygen Radicals in Biological Systems Part B: Oxygen Radicals and Antioxidants*; Academic Press: New York, 1990; Vol. 186, pp 1–85.
- (16). Gaetke LM; Chow CK Copper Toxicity, Oxidative Stress, and Antioxidant Nutrients. *Toxicology* 2003, 189 (1), 147–163. [PubMed: 12821289]

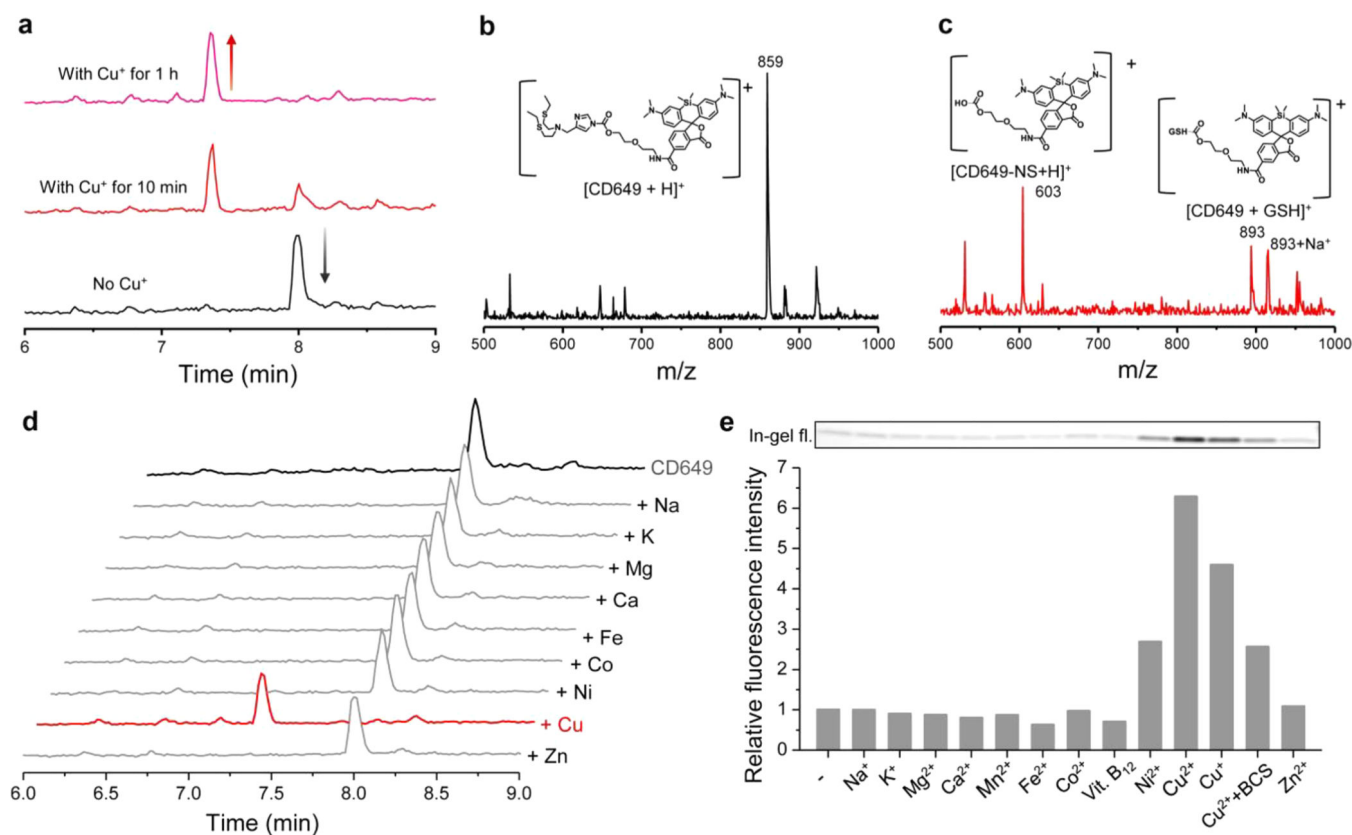
- (17). Brady DC; Crowe MS; Turski ML; Hobbs GA; Yao X; Chaikuad A; Knapp S; Xiao K; Campbell SL; Thiele DJ; Counter CM Copper Is Required for Oncogenic BRAF Signalling and Tumorigenesis. *Nature* 2014, 509 (7501), 492–496. [PubMed: 24717435]
- (18). Chung CY-S; Posimo JM; Lee S; Tsang T; Davis JM; Brady DC; Chang CJ Activity-Based Ratiometric FRET Probe Reveals Oncogene-Driven Changes in Labile Copper Pools Induced by Altered Glutathione Metabolism. *Proc. Natl. Acad. Sci. U. S. A* 2019, 116 (37), 18285–18294. [PubMed: 31451653]
- (19). Tsang T; Posimo JM; Gudiel AA; Cicchini M; Feldser DM; Brady DC Copper Is an Essential Regulator of the Autophagic Kinases ULK1/2 to Drive Lung Adenocarcinoma. *Nat. Cell Biol* 2020, 22, 412–424.
- (20). Fox JH; Kama JA; Lieberman G; Chopra R; Dorsey K; Chopra V; Volitakis I; Cherny RA; Bush AI; Hersch S Mechanisms of Copper Ion Mediated Huntington's Disease Progression. *PLoS One* 2007, 2 (3), No. e334. [PubMed: 17396163]
- (21). Desai V; Kaler SG Role of Copper in Human Neurological Disorders. *Am. J. Clin. Nutr* 2008, 88 (3), 855S–858S. [PubMed: 18779308]
- (22). Xiao G; Fan Q; Wang X; Zhou B Huntington Disease Arises from a Combinatory Toxicity of Polyglutamine and Copper Binding. *Proc. Natl. Acad. Sci. U. S. A* 2013, 110 (37), 14995–15000. [PubMed: 23980182]
- (23). Hare DJ; New EJ; de Jonge MD; McColl G Imaging Metals in Biology: Balancing Sensitivity, Selectivity and Spatial Resolution. *Chem. Soc. Rev* 2015, 44 (17), 5941–5958. [PubMed: 26505053]
- (24). Savelieff MG; Nam G; Kang J; Lee HJ; Lee M; Lim MH Development of Multifunctional Molecules as Potential Therapeutic Candidates for Alzheimer's Disease, Parkinson's Disease, and Amyotrophic Lateral Sclerosis in the Last Decade. *Chem. Rev* 2019, 119 (2), 1221–1322. [PubMed: 30095897]
- (25). Barnes N; Tsvikovskii R; Tsvikovaia N; Lutsenko S The Copper-Transporting ATPases, Menkes and Wilson Disease Proteins, Have Distinct Roles in Adult and Developing Cerebellum. *J. Biol. Chem* 2005, 280 (10), 9640–9645. [PubMed: 15634671]
- (26). Kaler SG ATP7A-Related Copper Transport Diseases-Emerging Concepts and Future Trends. *Nat. Rev. Neurol* 2011, 7 (1), 15–29. [PubMed: 21221114]
- (27). Fieten H; Gill Y; Martin AJ; Concilli M; Dirksen K; van Steenbeek FG; Spee B; van den Ingh TSGAM; Martens ECCP; Festa P; et al. The Menkes and Wilson Disease Genes Counteract in Copper Toxicosis in Labrador Retrievers: A New Canine Model for Copper-Metabolism Disorders. *Dis. Models & Mech* 2016, 9 (1), 25–38.
- (28). Jia S; Ramos-Torres KM; Kolemen S; Ackerman CM; Chang CJ Tuning the Color Palette of Fluorescent Copper Sensors through Systematic Heteroatom Substitution at Rhodol Cores. *ACS Chem. Biol* 2018, 13 (7), 1844–1852. [PubMed: 29112372]
- (29). Domaille DW; Que EL; Chang CJ Synthetic Fluorescent Sensors for Studying the Cell Biology of Metals. *Nat. Chem. Biol* 2008, 4 (3), 168–175. [PubMed: 18277978]
- (30). Aron AT; Ramos-Torres KM; Cotruvo JA; Chang CJ Recognition- and Reactivity-Based Fluorescent Probes for Studying Transition Metal Signaling in Living Systems. *Acc. Chem. Res* 2015, 48 (8), 2434–2442. [PubMed: 26215055]
- (31). Carter KP; Young AM; Palmer AE Fluorescent Sensors for Measuring Metal Ions in Living Systems. *Chem. Rev* 2014, 114 (8), 4564–4601. [PubMed: 24588137]
- (32). Zeng L; Miller EW; Pralle A; Isacoff EY; Chang CJ A Selective Turn-On Fluorescent Sensor for Imaging Copper in Living Cells. *J. Am. Chem. Soc* 2006, 128 (1), 10–11. [PubMed: 16390096]
- (33). Cotruvo JA Jr.; Aron AT; Ramos-Torres KM; Chang CJ Synthetic Fluorescent Probes for Studying Copper in Biological Systems. *Chem. Soc. Rev* 2015, 44 (13), 4400–4414. [PubMed: 25692243]
- (34). Ackerman CM; Lee S; Chang CJ Analytical Methods for Imaging Metals in Biology: From Transition Metal Metabolism to Transition Metal Signaling. *Anal. Chem* 2017, 89 (1), 22–41. [PubMed: 27976855]

- (35). Iovan DA; Jia S; Chang CJ Inorganic Chemistry Approaches to Activity-Based Sensing: From Metal Sensors to Bioorthogonal Metal Chemistry. *Inorg. Chem* 2019, 58 (20), 13546–13560. [PubMed: 31185541]
- (36). Fahrni CJ Synthetic Fluorescent Probes for Monovalent Copper. *Curr. Opin. Chem. Biol* 2013, 17 (4), 656–662. [PubMed: 23769869]
- (37). Yang L; McRae R; Henary MM; Patel R; Lai B; Vogt S; Fahrni CJ Imaging of the Intracellular Topography of Copper with a Fluorescent Sensor and by Synchrotron X-Ray Fluorescence Microscopy. *Proc. Natl. Acad. Sci. U. S. A* 2005, 102 (32), 11179–11184. [PubMed: 16061820]
- (38). Lin W; Yuan L; Tan W; Feng J; Long L Construction of Fluorescent Probes Via Protection/Deprotection of Functional Groups: A Ratiometric Fluorescent Probe for Cu<sup>2+</sup>. *Chem. - Eur. J* 2009, 15 (4), 1030–1035. [PubMed: 19053103]
- (39). Zhou Y; Wang F; Kim Y; Kim S-J; Yoon J Cu<sup>2+</sup>-Selective Ratiometric and “Off-On” Sensor Based on the Rhodamine Derivative Bearing Pyrene Group. *Org. Lett* 2009, 11 (19), 4442–4445. [PubMed: 19775186]
- (40). Taki M; Iyoshi S; Ojida A; Hamachi I; Yamamoto Y Development of Highly Sensitive Fluorescent Probes for Detection of Intracellular Copper(I) in Living Systems. *J. Am. Chem. Soc* 2010, 132 (17), 5938–5939. [PubMed: 20377254]
- (41). Domaille DW; Zeng L; Chang CJ Visualizing Ascorbate-Triggered Release of Labile Copper within Living Cells Using a Ratiometric Fluorescent Sensor. *J. Am. Chem. Soc* 2010, 132 (4), 1194–1195. [PubMed: 20052977]
- (42). Dodani SC; Leary SC; Cobine PA; Winge DR; Chang CJ A Targetable Fluorescent Sensor Reveals That Copper-Deficient SCO1 and SCO2 Patient Cells Prioritize Mitochondrial Copper Homeostasis. *J. Am. Chem. Soc* 2011, 133 (22), 8606–8616. [PubMed: 21563821]
- (43). Hirayama T; Van de Bittner GC; Gray LW; Lutsenko S; Chang CJ Near-Infrared Fluorescent Sensor for in Vivo Copper Imaging in a Murine Wilson Disease Model. *Proc. Natl. Acad. Sci. U. S. A* 2012, 109 (7), 2228–2233. [PubMed: 22308360]
- (44). Shen C; Kolanowski JL; Tran CM-N; Kaur A; Akerfeldt MC; Rahme MS; Hambley TW; New EJ A Ratiometric Fluorescent Sensor for the Mitochondrial Copper Pool. *Metallomics* 2016, 8 (9), 915–919. [PubMed: 27550322]
- (45). Park SY; Kim W; Park S-H; Han J; Lee J; Kang C; Lee MH An Endoplasmic Reticulum-Selective Ratiometric Fluorescent Probe for Imaging a Copper Pool. *Chem. Commun* 2017, 53 (32), 4457–4460.
- (46). Giuffrida ML; Trusso Sfrassetto G; Satriano C; Zimbone S; Tomaselli GA; Copani A; Rizzarelli E A New Ratiometric Lysosomal Copper(II) Fluorescent Probe To Map a Dynamic Metallome in Live Cells. *Inorg. Chem* 2018, 57 (5), 2365–2368. [PubMed: 29431435]
- (47). Morgan MT; Bourassa D; Harankhedkar S; McCallum AM; Zlatic SA; Calvo JS; Meloni G; Faundez V; Fahrni CJ Ratiometric Two-Photon Microscopy Reveals Attomolar Copper Buffering in Normal and Menkes Mutant Cells. *Proc. Natl. Acad. Sci. U. S. A* 2019, 116 (25), 12167–12172. [PubMed: 31160463]
- (48). Que EL; Chang CJ Responsive Magnetic Resonance Imaging Contrast Agents as Chemical Sensors for Metals in Biology and Medicine. *Chem. Soc. Rev* 2010, 39 (1), 51–60. [PubMed: 20023836]
- (49). Pierre VC; Harris SM; Pailloux SL Comparing Strategies in the Design of Responsive Contrast Agents for Magnetic Resonance Imaging: A Case Study with Copper and Zinc. *Acc. Chem. Res* 2018, 51 (2), 342–351. [PubMed: 29356506]
- (50). Que EL; Chang CJ A Smart Magnetic Resonance Contrast Agent for Selective Copper Sensing. *J. Am. Chem. Soc* 2006, 128 (50), 15942–15943. [PubMed: 17165700]
- (51). Que EL; Gianolio E; Baker SL; Wong AP; Aime S; Chang CJ Copper-Responsive Magnetic Resonance Imaging Contrast Agents. *J. Am. Chem. Soc* 2009, 131 (24), 8527–8536. [PubMed: 19489557]
- (52). Que EL; Gianolio E; Baker SL; Aime S; Chang CJ A Copper-Activated Magnetic Resonance Imaging Contrast Agent with Improved Turn-on Relaxivity Response and Anion Compatibility. *Dalton Trans.* 2010, 39 (2), 469–476.

- (53). Que EL; New EJ; Chang CJ A Cell-Permeable Gadolinium Contrast Agent for Magnetic Resonance Imaging of Copper in a Menkes Disease Model. *Chem. Sci* 2012, 3 (6), 1829–1834. [PubMed: 25431649]
- (54). Smolensky ED; Marja ska M; Pierre VC A Responsive Particulate MRI Contrast Agent for Copper(I): A Cautionary Tale. *Dalton Trans.* 2012, 41 (26), 8039–8046. [PubMed: 22585342]
- (55). Weitz EA; Lewandowski C; Smolensky ED; Marja ska M; Pierre VC A Magnetoplasmonic Imaging Agent for Copper(I) with Dual Response by MRI and Dark Field Microscopy. *ACS Nano* 2013, 7 (7), 5842–5849. [PubMed: 23746216]
- (56). Paranawithana NN; Martins AF; Clavijo Jordan V; Zhao P; Chirayil S; Meloni G; Sherry AD A Responsive Magnetic Resonance Imaging Contrast Agent for Detection of Excess Copper(II) in the Liver In Vivo. *J. Am. Chem. Soc* 2019, 141 (28), 11009–11018. [PubMed: 31268706]
- (57). Heffern MC; Park HM; Au-Yeung HY; Van de Bittner GC; Ackerman CM; Stahl A; Chang CJ In Vivo Bioluminescence Imaging Reveals Copper Deficiency in a Murine Model of Nonalcoholic Fatty Liver Disease. *Proc. Natl. Acad. Sci. U. S. A* 2016, 113 (50), 14219–14224. [PubMed: 27911810]
- (58). Chang CJ Bioinorganic Life and Neural Activity: Toward a Chemistry of Consciousness? *Acc. Chem. Res* 2017, 50 (3), 535–538. [PubMed: 28945425]
- (59). Krishnamoorthy L; Cotruvo JA Jr; Chan J; Kaluarachchi H; Muchenditsi A; Pendyala VS; Jia S; Aron AT; Ackerman CM; Wal MNV; Guan T; Smaga LP; Farhi SL; New EJ; Lutsenko S; Chang CJ Copper Regulates Cyclic-AMP-Dependent Lipolysis. *Nat. Chem. Biol* 2016, 12 (8), 586–592. [PubMed: 27272565]
- (60). Maity D; Kumar V; Govindaraju T Reactive Probes for Ratiometric Detection of Co<sup>2+</sup> and Cu<sup>+</sup> Based on Excited-State Intramolecular Proton Transfer Mechanism. *Org. Lett* 2012, 14 (23), 6008–6011. [PubMed: 23194428]
- (61). Taki M; Akaoka K; Mitsui K; Yamamoto Y A Mitochondria-Targeted Turn-on Fluorescent Probe Based on a Rhodol Platform for the Detection of Copper(I). *Org. Biomol. Chem* 2014, 12 (27), 4999–5005. [PubMed: 24887562]
- (62). Maity D; Raj A; Karthigeyan D; Kundu TK; Govindaraju T A Switch-on near-Infrared Fluorescence-Ready Probe for Cu(I): Live Cell Imaging. *Supramol. Chem* 2015, 27 (9), 589–594.
- (63). Hu Z; Hu J; Wang H; Zhang Q; Zhao M; Brommesson C; Tian Y; Gao H; Zhang X; Uvdal K A TPA-Caged Precursor of (Imino)Coumarin for “Turn-on” Fluorogenic Detection of Cu<sup>+</sup>. *Anal. Chim. Acta* 2016, 933, 189–195. [PubMed: 27497012]
- (64). Chan J; Dodani SC; Chang CJ Reaction-Based Small-Molecule Fluorescent Probes for Chemoselective Bioimaging. *Nat. Chem* 2012, 4 (12), 973–984. [PubMed: 23174976]
- (65). Bruemmer KJ; Crossley SWM; Chang CJ Activity-Based Sensing: A Synthetic Methods Approach for Selective Molecular Imaging and Beyond. *Angew. Chem., Int. Ed* 2020, 59, 13734.
- (66). Fujishima S; Yasui R; Miki T; Ojida A; Hamachi I Ligand-Directed Acyl Imidazole Chemistry for Labeling of Membrane-Bound Proteins on Live Cells. *J. Am. Chem. Soc* 2012, 134 (9), 3961–3964. [PubMed: 22352855]
- (67). Miki T; Awa M; Nishikawa Y; Kiyonaka S; Wakabayashi M; Ishihama Y; Hamachi I A Conditional Proteomics Approach to Identify Proteins Involved in Zinc Homeostasis. *Nat. Methods* 2016, 13 (11), 931–937. [PubMed: 27617391]
- (68). Matsuo K; Hamachi I Ligand-Directed Tosyl and Acyl Imidazole Chemistry In Chemoselective and Bioorthogonal Ligation Reactions; Algar WR, Dawson PE, Medintz IL, Eds.; Wiley-VCH Verlag GmbH & Co. KGaA: Hoboken, NJ, 2017; pp 147–163.
- (69). Zhu H; Tamura T; Hamachi I Chemical Proteomics for Subcellular Proteome Analysis. *Curr. Opin. Chem. Biol* 2019, 48, 1–7. [PubMed: 30170243]
- (70). Tamura T; Hamachi I Chemistry for Covalent Modification of Endogenous/Native Proteins: From Test Tubes to Complex Biological Systems. *J. Am. Chem. Soc* 2019, 141 (7), 2782–2799. [PubMed: 30592612]
- (71). Nishikawa Y; Miki T; Awa M; Kuwata K; Tamura T; Hamachi I Development of a Nitric Oxide-Responsive Labeling Reagent for Proteome Analysis of Live Cells. *ACS Chem. Biol* 2019, 14 (3), 397–404. [PubMed: 30715847]

- (72). Sakamoto S; Hamachi I Recent Progress in Chemical Modification of Proteins. *Anal. Sci* 2019, 35 (1), 5–27. [PubMed: 30318491]
- (73). Palmer AE; Tsien RY Measuring Calcium Signaling Using Genetically Targetable Fluorescent Indicators. *Nat. Protoc* 2006, 1 (3), 1057–1065. [PubMed: 17406387]
- (74). Nolan EM; Lippard SJ Small-Molecule Fluorescent Sensors for Investigating Zinc Metalloneurochemistry. *Acc. Chem. Res* 2009, 42 (1), 193–203. [PubMed: 18989940]
- (75). Dean KM; Qin Y; Palmer AE Visualizing Metal Ions in Cells: An Overview of Analytical Techniques, Approaches, and Probes. *Biochim. Biophys. Acta, Mol. Cell Res* 2012, 1823 (9), 1406–1415.
- (76). Miller EW; Zeng L; Domaille DW; Chang CJ Preparation and Use of Coppersensor-1, a Synthetic Fluorophore for Live-Cell Copper Imaging. *Nat. Protoc* 2006, 1 (2), 824–827. [PubMed: 17406313]
- (77). Hong-Hermesdorf A; Miethke M; Gallaher SD; Kropat J; Dodani SC; Chan J; Barupala D; Domaille DW; Shirasaki DI; Loo JA; Weber PK; Pett-Ridge J; Stemmler TL; Chang CJ; Merchant SS Subcellular Metal Imaging Identifies Dynamic Sites of Cu Accumulation in *Chlamydomonas*. *Nat. Chem. Biol* 2014, 10 (12), 1034–1042. [PubMed: 25344811]
- (78). Lee S; Barin G; Ackerman CM; Muchenditsi A; Xu J; Reimer JA; Lutsenko S; Long JR; Chang CJ Copper Capture in a Thioether-Functionalized Porous Polymer Applied to the Detection of Wilson's Disease. *J. Am. Chem. Soc* 2016, 138 (24), 7603–7609. [PubMed: 27285482]
- (79). Lukinavicius G; Umezawa K; Olivier N; Honigsmann A; Yang G; Plass T; Mueller V; Reymond L; Correa IR Jr.; Luo Z-G; et al. A Near-Infrared Fluorophore for Live-Cell Super-Resolution Microscopy of Cellular Proteins. *Nat. Chem* 2013, 5 (2), 132–139. [PubMed: 23344448]
- (80). Wagner BD The Use of Coumarins as Environmentally-Sensitive Fluorescent Probes of Heterogeneous Inclusion Systems. *Molecules* 2009, 14 (1), 210–237. [PubMed: 19127249]
- (81). Castner EW; Kennedy D; Cave RJ Solvent as Electron Donor: Donor/Acceptor Electronic Coupling Is a Dynamical Variable. *J. Phys. Chem. A* 2000, 104 (13), 2869–2885.
- (82). Petris MJ; Mercer JF; Culvenor JG; Lockhart P; Gleeson PA; Camakaris J Ligand-Regulated Transport of the Menkes Copper P-Type ATPase Efflux Pump from the Golgi Apparatus to the Plasma Membrane: A Novel Mechanism of Regulated Trafficking. *EMBO J.* 1996, 15 (22), 6084–6095. [PubMed: 8947031]
- (83). Camakaris J; Voskoboinik I; Mercer JF Molecular Mechanisms of Copper Homeostasis. *Biochem. Biophys. Res. Commun* 1999, 261 (2), 225–232. [PubMed: 10425169]
- (84). Linz R; Lutsenko S Copper-Transporting ATPases ATP7A and ATP7B: Cousins, Not Twins. *J. Bioenerg. Biomembr* 2007, 39 (5–6), 403–407. [PubMed: 18000748]
- (85). Gupta A; Lutsenko S Human Copper Transporters: Mechanism, Role in Human Diseases and Therapeutic Potential. *Future Med. Chem* 2009, 1 (6), 1125–1142. [PubMed: 20454597]
- (86). Lutsenko S; Bhattacharjee A; Hubbard AL Copper Handling Machinery of the Brain. *Metallomics* 2010, 2 (9), 596–608. [PubMed: 21072351]
- (87). Gaier ED; Eipper BA; Mains RE Copper Signaling in the Mammalian Nervous System: Synaptic Effects. *J. Neurosci. Res* 2012, 91 (1), 2–19. [PubMed: 23115049]
- (88). Zimbrean PC; Schilsky ML Psychiatric Aspects of Wilson Disease: A Review. *Gen. Hosp. Psychiatry* 2014, 36 (1), 53–62. [PubMed: 24120023]
- (89). Kardos J; Héja L; Simon Á; Jablonkai I; Kovács R; Jemnitz K Copper Signalling: Causes and Consequences. *Cell Commun. Signaling* 2018, 16 (1), 71.
- (90). Campbell A The Role of Aluminum and Copper on Neuroinflammation and Alzheimer's Disease. *J. Alzheimer's Dis* 2006, 10 (2–3), 165–172. [PubMed: 17119285]
- (91). Choo XY; Alukaidey L; White AR; Grubman A Neuroinflammation and Copper in Alzheimer's Disease. *Int. J. Alzheimer's Dis* 2013, 2013, 145345 (accessed Dec 18, 2019). [PubMed: 24369524]
- (92). Dusek P; Roos PM; Litwin T; Schneider SA; Flaten TP; Aaseth J The Neurotoxicity of Iron, Copper and Manganese in Parkinson's and Wilson's Diseases. *J. Trace Elem. Med. Biol* 2015, 31, 193–203. [PubMed: 24954801]

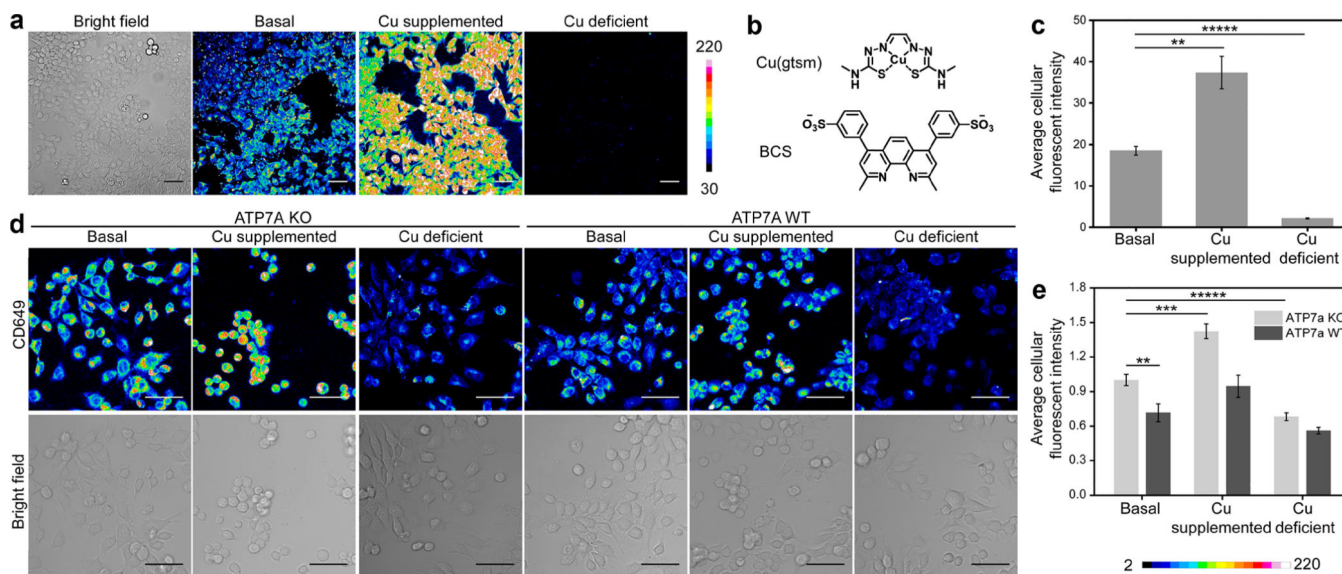
- (93). Bulcke F; Dringen R; Scheiber IF Neurotoxicity of Copper In Neurotoxicity of Metals; Aschner M, Costa LG, Eds.; Advances in Neurobiology; Springer International Publishing: Cham, 2017; pp 313–343.
- (94). Brosenitsch TA; Katz DM Physiological Patterns of Electrical Stimulation Can Induce Neuronal Gene Expression by Activating N-Type Calcium Channels. *J. Neurosci* 2001, 21 (8), 2571–2579. [PubMed: 11306610]
- (95). Ghasemi-Mobarakeh L; Prabhakaran MP; Morshed M; Nasr-Esfahani MH; Baharvand H; Kiani S; Al-Deyab SS; Ramakrishna S Application of Conductive Polymers, Scaffolds and Electrical Stimulation for Nerve Tissue Engineering. *J. Tissue Eng. Regener. Med* 20115 (4), e17–e35.
- (96). Reemst K; Noctor SC; Lucassen PJ; Hol EM The Indispensable Roles of Microglia and Astrocytes during Brain Development. *Front. Hum. Neurosci* 2016, 10, 566. [PubMed: 27877121]
- (97). Dringen R; Scheiber IF; Mercer JF B. Copper Metabolism of Astrocytes. *Front. Aging Neurosci* 2013, 5, 9. [PubMed: 23503037]
- (98). Saijo K; Crotti A; Glass CK Regulation of Microglia Activation and Deactivation by Nuclear Receptors. *Glia* 2013, 61 (1), 104–111. [PubMed: 22987512]
- (99). Chung W-S; Allen NJ; Eroglu C Astrocytes Control Synapse Formation, Function, and Elimination. *Cold Spring Harbor Perspect. Biol* 2015, 7 (9), No. a020370.
- (100). Niciu MJ; Ma X-M; El Meskini R; Ronnett GV; Mains RE; Eipper BA Developmental Changes in the Expression of ATP7A during a Critical Period in Postnatal Neurodevelopment. *Neuroscience* 2006, 139 (3), 947–964. [PubMed: 16549268]
- (101). Zheng Z; White C; Lee J; Peterson TS; Bush AI; Sun GY; Weisman GA; Petris MJ Altered Microglial Copper Homeostasis in a Mouse Model of Alzheimer’s Disease. *J. Neurochem* 2010, 114 (6), 1630–1638. [PubMed: 20626553]
- (102). Telianidis J; Hung YH; Materia S; La Fontaine S Role of the P-Type ATPases, ATP7A and ATP7B in Brain Copper Homeostasis. *Front. Aging Neurosci* 2013, 5, 44. [PubMed: 23986700]



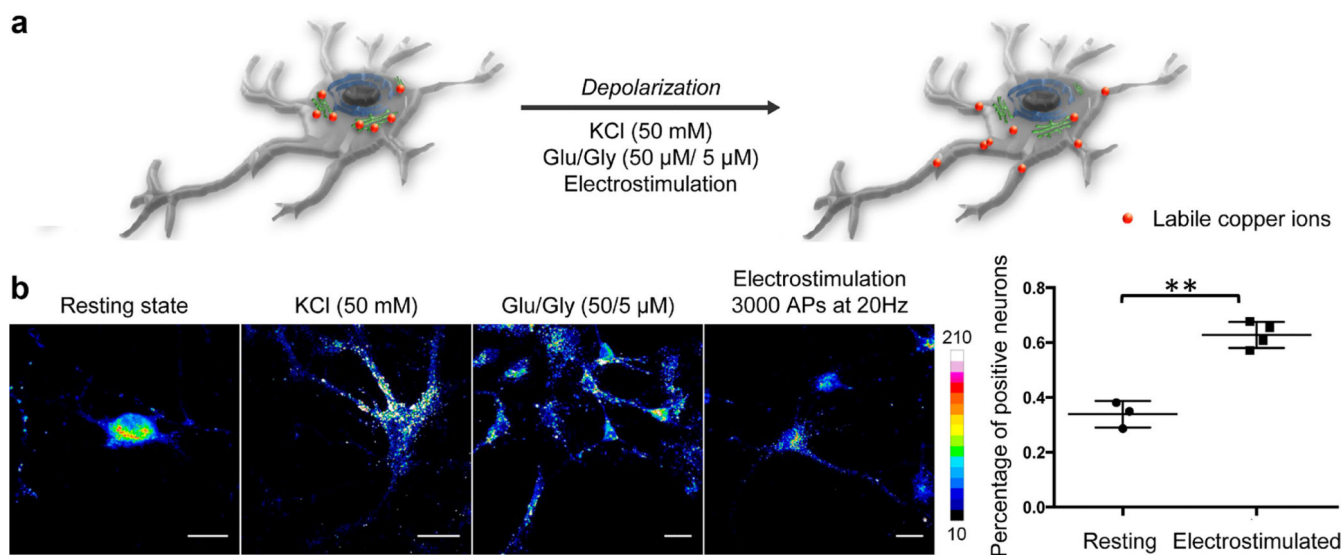
**Figure 1.**

Copper reactivity and selectivity of CD probes in aqueous buffer solutions. (a) LC chromatograms of the reaction between 5  $\mu\text{M}$  CD649 and 10  $\mu\text{M}$  Cu(I) in PBS containing 25  $\mu\text{M}$  L-serine methyl ester and 2 mM GSH for 1 h, showing the complete conversion of CD649. (b) The mass of intact CD649 probe was detected at a retention time of 8.0 min in the absence of Cu(I). (c) The copper-responsive reaction products of CD649 with Cu(I)/2 mM GSH are detected at a retention time of 7.4 min. (d) LC chromatograms of 5  $\mu\text{M}$  CD649 (top trace, black), 5  $\mu\text{M}$  CD649 incubated with 10  $\mu\text{M}$  Cu(I) (red trace) for 30 min, and other biologically relevant metals at 10  $\mu\text{M}$  ( $\text{Na}^+$ ,  $\text{K}^+$ ,  $\text{Mg}^{2+}$ ,  $\text{Ca}^{2+}$ ,  $\text{Fe}^{3+}$ ,  $\text{Co}^{2+}$ ,  $\text{Ni}^{2+}$ ,  $\text{Cu}^+$ , and  $\text{Zn}^{2+}$ , gray traces) for 30 min in PBS in the presence of 25  $\mu\text{M}$  L-serine methyl ester and 2 mM GSH. The LC data support that CD649 shows high selective reactivity toward copper ions. (e) In-gel fluorescence images and integrated fluorescence intensities of CD649 and lysozyme as a model protein for activity-based sensing of copper via copper-induced bioconjugation. Lysozyme was preincubated with biologically relevant metal ions for 5 min (s-block metal ions at 1 mM, d-block metal ions at 10  $\mu\text{M}$ , BCS at 50  $\mu\text{M}$ ), followed by incubation with 1  $\mu\text{M}$  CD649 at room temperature for 2 h. In-gel fluorescence for SDS-PAGE was scanned by ChemiDoc MP and signal intensity was analyzed by ImageJ.



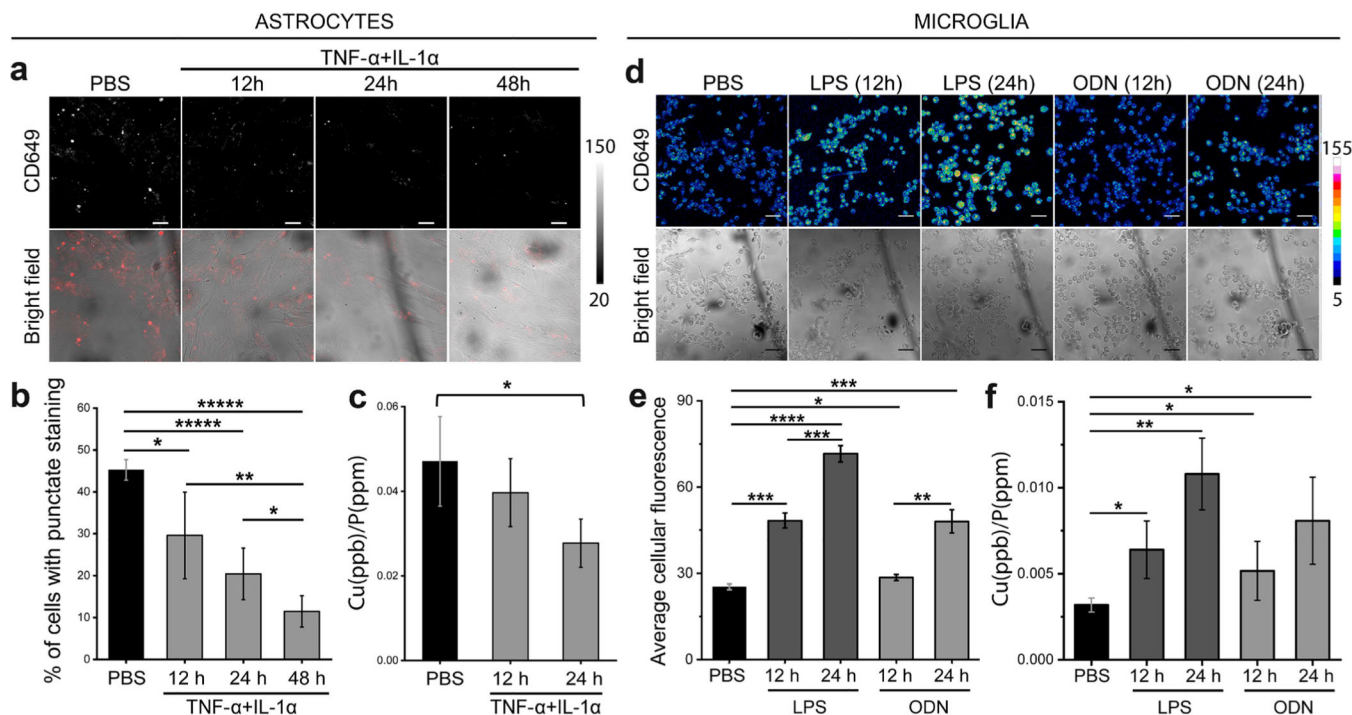
**Figure 2.**

Fluorescence imaging of labile copper pools in live HEK293T cells and MEF cells with wild-type or altered expression levels of the copper transporter protein ATP7A using CD649. (a) Confocal fluorescence microscopic images of HEK 293T cells treated with 1  $\mu\text{M}$  CD649 alone, CD649 and 2  $\mu\text{M}$  Cu(gtsm) for Cu supplementation, or CD649 and 200  $\mu\text{M}$  BCS for Cu deficiency. The cells were incubated with 2  $\mu\text{M}$  Cu(gtsm) for 2 h or 200  $\mu\text{M}$  BCS in DMEM/10% FBS medium overnight and washed with DMEM/10% FBS and PBS, followed by incubation with 1  $\mu\text{M}$  CD649 in DPBS solution and then imaged after 15 min. (b) Chemical structures of Cu(gtsm) and BCS. (c) Normalized cellular fluorescence intensities of the HEK 293T cells as determined using ImageJ, showing a turn-on response when treated with Cu(gtsm) and a turn-off response in the presence of BCS. Error bars denote standard derivation (SD;  $n = 3$ ). Scale bar = 50  $\mu\text{m}$ . (d) Confocal fluorescence microscopic images of MEF ATP7A WT or KO cells treated with DMSO vehicle, 2  $\mu\text{M}$  Cu(gtsm) for 30 min, or 200  $\mu\text{M}$  BCS for overnight in DMEM/10% FBS and washed with DMEM/10% FBS and PBS, followed by incubation with 1  $\mu\text{M}$  CD649 in DPBS and then imaged after 15 min. (e) Average cellular fluorescence intensity of CD649 determined from experiments performed in triplicate with  $\lambda_{\text{ex}} = 633 \text{ nm}$ . Error bars denote standard derivation (SD;  $n = 3$ ). Scale bar = 50  $\mu\text{m}$ . \* $p < 0.05$ , \*\* $p < 0.01$ , \*\*\* $p < 0.001$ , and \*\*\*\* $p < 0.0001$ .



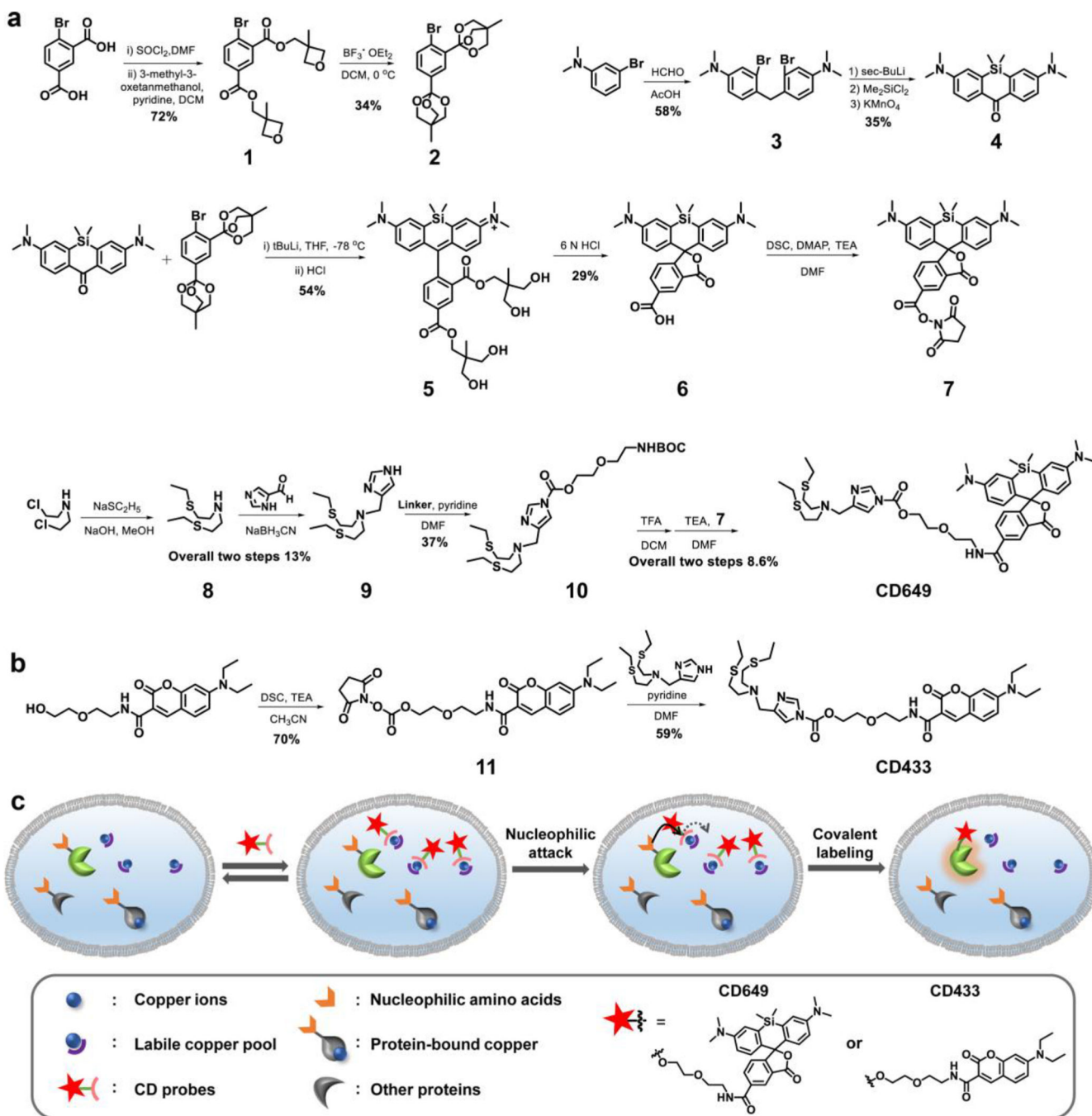
**Figure 3.**

CD649 can image translocation of labile copper pools from cell bodies to projections in cultured primary neurons upon chemical/electrical stimulation. (a) Depiction of observed copper redistributions in neurons before and after depolarization by various stimuli. (b) Fluorescence images of primary cultured hippocampal neurons stained with 1  $\mu$ M CD649 in the resting state and after depolarization by KCl (50 mM), 50  $\mu$ M glutamate and 5  $\mu$ M glycine (Glu/Gly), or electrostimulation (3000 evoked action potentials at a frequency of 20 Hz). (c) Percentage of neurons showing copper pools residing at distances greater than one cell body away from soma. The percentage of such neurons increases significantly after depolarization. Scale bar is 20  $\mu$ m. \*\* $p$  < 0.01.



**Figure 4.**

Fluorescence imaging of labile copper pools in human astrocytes (HA) and microglia SIMA9 under various inflammatory responses using CD649. (a) Confocal fluorescence microscopic images of astrocytes treated by PBS control or a combination of TNF- $\alpha$  and IL-1 $\alpha$  (both at 20 ng/mL) up to 48 h and stained with 5  $\mu$ M CD649 in HBSS for 30 min, fixed and then imaged. Scale bar = 25  $\mu$ m. (b) Average cellular fluorescence intensity of CD649 determined from experiments in (a) performed in triplicate with  $\lambda_{\text{ex}}$  = 633 nm. Error bars denote standard deviation (SD;  $n$  = 3) (c) ICP-MS measurement to determine total cellular  $^{63}\text{Cu}$  levels in astrocytes under TNF- $\alpha$  and IL-1 $\alpha$  inflammatory stimuli (with normalization of different cell numbers by total cellular  $^{31}\text{P}$  level). Error bars denote SD;  $n$  = 2. (d) Confocal fluorescence microscopic images of microglia stimulated by PBS control, lipopolysaccharide (LPS, 0.1  $\mu\text{g}/\text{mL}$ ), or CpG oligodeoxynucleotides (ODN, 5  $\mu\text{g}/\text{mL}$ ). Five  $\mu\text{M}$  CD649 in HBSS was incubated subsequently for 30 min and then imaged after fixation. Scale bar = 25  $\mu\text{m}$ . (e) Average cellular fluorescence intensity of CD649 determined from experiments in (d) performed in triplicate with  $\lambda_{\text{ex}}$  = 633 nm. Error bars denote SD;  $n$  = 5 different images from the triplicate experiments. (f) ICP-MS measurement to determine total cellular  $^{63}\text{Cu}$  levels in microglia under various inflammatory stimuli (with normalization of different cell numbers by total cellular  $^{31}\text{P}$  level). Error bars denote SD;  $n$  = 2. \* $p$  < 0.05, \*\* $p$  < 0.01, \*\*\* $p$  < 0.001, and \*\*\*\* $p$  < 0.0001.

**Scheme 1.**

Synthesis of (a) CD649 and (b) CD433; (c) Schematic Cartoon Showing the Working Principle of CD Dyes for Fluorescent Labeling of Proximal Proteins at Sites of Elevated Labile Copper